

Radiative Decays of Vector Mesons with Light-Cone Sum Rules

Zhi Jun Wang^{1,*}, Di Gao^{1,2,3,†}, Kai Kai Zhang^{1,‡}, Yuan Yuan Ma^{1,§}, and Yan Jun Sun^{1,¶}

¹*Institute of Theoretical Physics,
College of Physics and Electronic Engineering,
Northwest Normal University,
Lanzhou 730070, China*
²*Institute of Modern Physics,
Chinese Academy of Sciences,
Lanzhou 730000, China*
³*Lebedev Physical Institute,
Russian Academy of Sciences,
Leninsky Prospekt 53, 119991, Moscow, Russia*

(Dated: November 26, 2025)

Hadronic electromagnetic form factors and radiative decay properties offer a crucial window into the nonperturbative dynamics of Quantum chromodynamics (QCD). In this work, we employ the light-cone sum rules (LCSR) method to systematically investigate the M1 radiative decay of vector mesons. Our study covers processes including $K^{*-} \rightarrow K^- \gamma$, $D^* \rightarrow D \gamma$, $B^* \rightarrow B \gamma$, $D_s^{*+} \rightarrow D_s^+ \gamma$, and $B_s^* \rightarrow B_s \gamma$, and further extends to the excited charmonium state $\psi(2S)$. Our calculations yield decay widths for K^* and $\psi(2S)$ that are in excellent agreement with experimental data. For the charm and bottom meson decays, where precise measurements are lacking, we provide theoretical predictions and compare them with other theoretical approaches. Most notably, our analysis reveals a universal linear dependence of the decay width on a function $A(x)$ in the logarithmic coordinate system, which originates from the two-body decay dynamics and the ratio of the initial and final state decay constants. This relationship holds for the ground state $V \rightarrow P \gamma$ processes here and suggests a broader applicability to radiative decays of ground-state vector mesons.

I. INTRODUCTION

Quantum Chromodynamics (QCD) is the fundamental theory describing the strong interaction. The property of asymptotic freedom enables the application of perturbative QCD in the high energy regime, leading to remarkable successes in describing both inclusive and exclusive processes at large momentum transfer. Nevertheless, investigating the properties of QCD in the non-

*Electronic address: 2023212251@nwnu.edu.cn

†Electronic address: digao@impcas.ac.cn

‡Electronic address: zhangkk314@outlook.com

§Electronic address: Mayuanyuan917@163.com

¶Corresponding author; Electronic address: sunyanjun@nwnu.edu.cn

perturbative domain represents a central challenge in modern particle physics. Electromagnetic transitions provide a crucial window into this domain. Among these, magnetic dipole (M1) transitions, where a spin-1 vector meson decays into a spin-0 pseudoscalar meson via photon emission, serve as powerful probes for investigating hadron structure. The corresponding transition form factors are pivotal for deepening our insight into nonperturbative QCD dynamics [1–5]. At present, the Particle Data Group (PDG) [6] has compiled extensive experimental data on hadron radiative decays. This highlights the demand for robust theoretical frameworks capable of interpreting these results and predicting new decay channels.

Currently, M1 radiative decays have been experimentally observed for numerous mesons. For example, for the ground state magnetic dipole (M1) radiative transition $K^{*-} \rightarrow K^-\gamma$, the decay width is 50.37 keV [6]. For the charm-containing processes $D^* \rightarrow D\gamma$ and $D_s^{*+} \rightarrow D_s^+\gamma$, only upper limits are available for the M1 radiative decay widths specifically 2.1 MeV and 1.9 MeV, respectively [7–10]. Recently, the latest data from the Beijing Spectrometer (BESIII) collaboration reported measurements of the branching fractions for $D^* \rightarrow D\gamma$ and $D_s^{*+} \rightarrow D_s^+\gamma$ as $(34.5 \pm 0.8 \pm 0.5)\%$ and $(93.57 \pm 0.38 \pm 0.22)\%$, respectively [11, 12]. However, although the M1 radiative decays of the B^* and B_s^* mesons have been experimentally observed, their decay widths still lack precise experimental measurements [6]. For the excited state magnetic dipole radiative transition $\psi(2S) \rightarrow \eta_c(2S)\gamma$, this transition poses a particular challenge due to the narrow phase space of $\eta_c(2S)$. Subsequent studies have confirmed that $\eta_c(2S)$ can be produced via radiative decay of $\psi(2S)$. The Crystal Ball group [13] reported an excess of $E_\gamma \simeq 91$ MeV gamma rays from inclusive $\psi(2S) \rightarrow X\gamma$ decays and interpreted this as possible evidence for the $\eta_c(2S)$ with mass 3594 ± 5 MeV/ c^2 . The Belle collaboration later observed the pseudoscalar meson $\eta_c(2S)$ in B meson decays [14]. Recently, the BESIII collaboration investigated the M1 transition in the decay $\psi(2S) \rightarrow \eta_c(2S)\gamma$, measuring the corresponding branching fraction as $\mathcal{B}(\psi(3686) \rightarrow \eta_c(2S)\gamma) = (5.2 \pm 0.3 \pm 0.5_{-1.4}^{+1.9}) \times 10^{-4}$, and the decay width as $\Gamma(\psi(3686) \rightarrow \eta_c(2S)\gamma) = 0.15_{-0.04}^{+0.06}$ keV [15]. Theoretically, a wide array of theoretical frameworks has been developed for M1 radiative decays, such as Godfrey-Isgur (GI) model [16–18], relativistic quark model [19], light-front quark model (LFQM) [20], light-cone quark model [21], meson loop corrections (IML) [22, 23], QCD sum rules (QCDSR) [24–27], lattice quantum chromodynamics (LQCD) [28–34], and light-cone sum rules (LCSR) [35–38]. Nevertheless, significant challenges persist in the study of radiative decays and related research areas, as exemplified by the $\rho - \pi$ puzzle [39–41] and several anomalous decay phenomena. Resolving these puzzles and advancing our fundamental understanding of hadronic structure and its underlying interaction mechanisms will necessitate sustained and concerted investigation on both experimental and theoretical fronts.

Light-cone sum rules (LCSR) is a non-perturbative method based on the first principles of QCD. It combines the operator product expansion (OPE) with a description of nonperturbative dynamics in terms of light-cone distribution amplitude (LCDA), and has been proven highly effective in calculating key nonperturbative parameters for exclusive processes [42, 43]. The method exhibits a comprehensive scope of applicability, enabling calculations of transition form factors [44–46], coupling constants [47], decay constants [48, 49], magnetic moments of multiquark states and other physical quantities [50–54]. In this work, we employ LCSR to carry out a systematic study of the M1 radiative decays of vector mesons (K^{*-} , B^* , B_s^* , D^* , D_s^{*+}) and extend the formalism

to the radiative transition of the excited charmonium state $\psi(2S) \rightarrow \eta_c(2S)\gamma$, thereby testing the applicability of LCSR to excited states. In addition to computing the transition form factors and decay widths and comparing them with existing data and other theoretical approaches, we have performed a comprehensive analysis of the systematics of these decays. Notably, we identify a universal linear relationship between the decay width and a specific kinematic function $A(x)$. This observed scaling may offer a fresh, unifying perspective on the systematics of radiative decays and could provide valuable insights into understanding broader hadronic anomalies, such as the $\rho - \pi$ puzzle, by revealing underlying universal dynamics in M1 transitions.

This work is organized as follows. Sec. II outlines the theoretical framework and details the derivation of the transition form factors within the light-cone sum rules. Sec. III presents the numerical results, discusses their physical implications, and compares them with available experimental data and other theoretical approaches. Finally, Sec. IV summarizes our findings and provides an outlook for future research.

II. FORM FACTOR WITH LCSR

A. Form Factor for K^* Transition

This section details the derivation of the transition form factors for the M1 radiative decays within the LCSR framework. We first present a comprehensive calculation for the process $K^{*-} \rightarrow K^- \gamma$. The formalism for other heavy-light meson transitions (D^* , B^* , D_s^* , B_s^*) follows an analogous procedure, with the final results summarized for brevity. Subsequently, we extend the formalism to the charmonium sector to address the excited state transition $\psi(2S) \rightarrow \eta_c(2S)\gamma$. For the $K^{*-} \rightarrow K^- \gamma$ decay channel, the following correlation function is employed

$$\Pi_{\mu\nu}(Q, q) = i \int d^4x e^{iq \cdot x} \langle K^-(Q) | T \{ J_\mu(x) J_\nu(0) \} | 0 \rangle, \quad (1)$$

here, Q is the four-momentum of the final-state K^- meson, q is the four-momentum of the outgoing photon, and the currents are defined as $J_\mu = \bar{s}(x)\gamma_\mu s(x)$ and $J_\nu = \bar{u}(x)\gamma_\nu s(x)$.

On the phenomenological side, a complete set of hadronic states sharing the same quantum numbers as the final states is inserted between the two currents, yielding

$$\begin{aligned} \Pi_{\mu\nu}(Q, q) = & i \int d^4x e^{iq \cdot x} \sum_n \int \frac{d^3\vec{P}_1}{(2\pi)^3 2E_1} \theta(x_0 - 0) e^{iQ \cdot x} e^{-iP_1 \cdot x} \langle K^-(Q) | \bar{s}(0)\gamma_\mu s(0) | n \rangle \langle n | \bar{u}(0)\gamma_\nu s(0) | 0 \rangle \\ & + i \int d^4x e^{iq \cdot x} \sum_n \int \frac{d^3\vec{P}_1}{(2\pi)^3 2E_1} \theta(0 - x_0) e^{iP_1 \cdot x} \langle K^-(Q) | \bar{u}(0)\gamma_\nu s(0) | n \rangle \langle n | \bar{s}(0)\gamma_\mu s(0) | 0 \rangle. \end{aligned} \quad (2)$$

Isolating the ground state contributions gives

$$\begin{aligned} \Pi_{\mu\nu}(Q, q) = & \frac{1}{m_{K^{*-}}^2 - (q + Q)^2} \langle K^-(Q) | \bar{s}(0)\gamma_\mu s(0) | K^{*-} \rangle \langle K^{*-} | \bar{u}(0)\gamma_\nu s(0) | 0 \rangle \\ & + \int_{s_0}^{\infty} ds \frac{\rho(Q^2, s)}{s - (Q + q)^2}, \end{aligned} \quad (3)$$

where s_0 is the threshold parameter that separates the ground state from excited states. Following Ref. [55], the matrix elements are parametrized as

$$\langle K^-(Q)|\bar{s}(0)\gamma_\mu s(0)|K^{*-}\rangle = \varepsilon_{\mu\alpha\beta\gamma} Q^\beta q^\alpha \varepsilon^{*\gamma} F_{VP} \frac{2}{m_{K^{*-}} + m_{K^-}}, \quad (4)$$

$$\langle K^{*-}|\bar{s}(0)\gamma_\nu s(0)|0\rangle = m_{K^{*-}} f_{K^{*-}} \varepsilon_\nu, \quad (5)$$

where, $m_{K^{*-}}$ is the mass of the K^{*-} meson, m_{K^-} is the mass of the K^- meson, $f_{K^{*-}}$ is the decay constant, ε_ν is the polarization vector, $\varepsilon_{\mu\alpha\beta\gamma}$ is a totally antisymmetric tensor and F_{VP} is the transition form factor. With these parameterizations, the correlator on the phenomenological side becomes

$$\begin{aligned} \Pi_{\mu\nu}(Q, q) &= \frac{1}{m_{K^{*-}}^2 - (Q+q)^2} \frac{2\varepsilon_{\mu\alpha\beta\gamma} Q^\beta q^\alpha \varepsilon^{*\gamma} F_{VP} m_{K^{*-}} f_{K^{*-}} \varepsilon_\nu}{m_{K^{*-}} + m_{K^-}} \\ &+ \int_{s_0}^{\infty} ds \frac{\rho(Q^2, s)}{s - (Q+q)^2}. \end{aligned} \quad (6)$$

On the theoretical side of the correlator, the operator product expansion (OPE) is employed. By substituting the propagator of s-quark $iS(0, x) = -i \int \frac{d^4k}{(2\pi)^4} e^{-ik \cdot x} \frac{m_s - \not{k} \gamma_5}{m_s^2 - k^2}$ into the correlation function, we obtain

$$\Pi_{\mu\nu}(Q, q) = i^2 \int d^4x e^{iqx} \int \frac{d^4k}{(2\pi)^4} e^{-ik \cdot x} \frac{-k^\alpha}{m_s^2 - k^2} \langle K^-(Q)|\bar{u}(x)\gamma_\mu \gamma_\alpha \gamma_\nu s(0)|0\rangle. \quad (7)$$

Since the light-cone distribution amplitude of K meson is defined as [56]

$$\langle K^-(Q)|\bar{u}(x)\gamma^\beta \gamma_5 s(0)|0\rangle = -iQ^\beta f_{K^-} \int_0^1 du e^{-iuQ \cdot x} \phi_{K^-}(u) + \text{higher twist terms}, \quad (8)$$

the correlation function is derived as

$$\Pi_{\mu\nu}(Q, q) = \varepsilon_{\mu\alpha\nu\beta} f_{K^-} Q^\beta q^\alpha \int_0^1 du \frac{\phi_{K^-}(u)}{m_s^2 - (q+uQ)^2}. \quad (9)$$

Applying the ‘‘quark-hadron duality’’ assumption to the hadronic spectral density in Eq. (6)

$$\int_0^\infty ds \frac{\rho^h(s)}{s - q^2} \simeq \frac{1}{\pi} \int_0^\infty ds \frac{\text{Im}\Pi^{\text{pert}}(s)}{s - q^2}. \quad (10)$$

and matching the theoretical side with the phenomenological side yields

$$\frac{F_{VP}}{m_{K^{*-}}^2 - (Q+q)^2} = -\frac{1}{2} \frac{m_{K^{*-}} + m_{K^-}}{m_{K^{*-}}} \frac{f_{K^-}}{f_{K^{*-}}} \int_\Delta^1 du \frac{\phi_{K^-}(u)}{m_s^2 - (uQ+q)^2}. \quad (11)$$

To suppress the contributions from higher excited states and the continuum, we apply the Borel transformation [42, 56, 57] to the 4-momenta $(Q+q)$ and $(uQ+q)$

$$\begin{aligned} \mathcal{B}_{M^2} \left[\frac{1}{m_{K^{*-}}^2 - (Q+q)^2} \right] &= \frac{1}{M^2} e^{-m_{K^{*-}}^2/M^2}, \\ \mathcal{B}_{M^2} \left[\frac{1}{m_s^2 - (uQ+q)^2} \right] &= \frac{1}{uM^2} e^{-\frac{1}{uM^2} [m_s^2 + u(1-u)Q^2 - (1-u)q^2]}. \end{aligned} \quad (12)$$

Finally, the transition form factor is obtained

$$F_{VP} = \frac{1}{2} \frac{m_{K^{*-}} + m_{K^-}}{m_{K^{*-}}} \frac{f_{K^-}}{f_{K^{*-}}} \int_{\Delta}^1 du \frac{\phi_{K^-}(u)}{u} e^{-\frac{1}{uM^2}[m_s^2 + u(1-u)m_{K^-}^2 + (1-u)P'^2] + \frac{m_{K^{*-}}^2}{M^2}}, \quad (13)$$

where $\Delta = \frac{1}{2m_{K^-}^2} \left[\sqrt{(s_0 - m_{K^-}^2 + P'^2)^2 + 4m_{K^-}^2(m_s^2 + P'^2)} - (s_0 - m_{K^-}^2 - q^2) \right]$ is the lower integration limit in Eq. (13), and the four-momenta are specified as $Q^2 = m_{K^-}^2$ and $P'^2 = -q^2$.

Through phenomenological and theoretical treatments of the correlation function, followed by matching procedures, the form factor for the $K^{*-} \rightarrow K^- \gamma$ process has been obtained. This methodology is universally applicable to other processes, and for $D^* \rightarrow D\gamma$, $B^* \rightarrow B\gamma$, $D_s^{*+} \rightarrow D_s^+ \gamma$ and $B_s^* \rightarrow B_s \gamma$, the form factors are

$$\begin{aligned} F_{VP} &= \frac{1}{2} \frac{m_{D^*} + m_D}{m_{D^*}} \frac{f_D}{f_{D^*}} \int_{\Delta}^1 du \frac{\phi_D(u)}{u} e^{-\frac{1}{uM^2}[m_c^2 + u(1-u)m_D^2 + (1-u)P'^2] + \frac{m_{D^*}^2}{M^2}}, \\ F_{VP} &= \frac{1}{2} \frac{m_{B^*} + m_B}{m_{B^*}} \frac{f_B}{f_{B^*}} \int_{\Delta}^1 du \frac{\phi_B(u)}{u} e^{-\frac{1}{uM^2}[m_b^2 + u(1-u)m_B^2 + (1-u)P'^2] + \frac{m_{B^*}^2}{M^2}}, \\ F_{VP} &= \frac{1}{2} \frac{m_{D_s^{*+}} + m_{D_s^+}}{m_{D_s^{*+}}} \frac{f_{D_s^+}}{f_{D_s^{*+}}} \int_{\Delta}^1 du \frac{\phi_{D_s^+}(u)}{u} e^{-\frac{1}{uM^2}[m_c^2 + u(1-u)m_{D_s^+}^2 + (1-u)P'^2] + \frac{m_{D_s^{*+}}^2}{M^2}}, \\ F_{VP} &= \frac{1}{2} \frac{m_{B_s^*} + m_{B_s}}{m_{B_s^*}} \frac{f_{B_s}}{f_{B_s^*}} \int_{\Delta}^1 du \frac{\phi_{B_s}(u)}{u} e^{-\frac{1}{uM^2}[m_b^2 + u(1-u)m_{B_s}^2 + (1-u)P'^2] + \frac{m_{B_s^*}^2}{M^2}}, \end{aligned} \quad (14)$$

where m_{D^*} (m_{B^*} , $m_{D_s^{*+}}$, $m_{B_s^*}$) is the mass of the initial state meson, m_D (m_B , $m_{D_s^+}$, m_{B_s}) is the mass of the final state meson, and f_{D^*} (f_{B^*} , $f_{D_s^{*+}}$, $f_{B_s^*}$) and f_D (f_B , $f_{D_s^+}$, f_{B_s}) are the decay constants of the initial and final state mesons, respectively. Additionally, m_c and m_b are the masses of the c-quark and the b-quark, respectively.

B. Form Factor for $\psi(2S)$ Transition

The LCSR method can also be applied to transitions involving excited states. We consider the M1 radiative decay $\psi(2S) \rightarrow \eta_c(2S)\gamma$. The correlation function is defined as

$$\Pi_{\mu\nu}(Q, q) = i \int d^4x e^{iq \cdot x} \langle \eta_c(2S)(Q) | T \{ J_{\mu}^c(x) J_{\nu}^c(0) \} | 0 \rangle, \quad (15)$$

where the electromagnetic currents of the c-quark are given by $J_{\mu}^c = \bar{c}(x)\gamma_{\mu}c(x)$ and $J_{\nu}^c = \bar{c}(x)\gamma_{\nu}c(x)$.

On the phenomenological side of the correlation function, we insert the hadron state $\sum_n |n\rangle\langle n|$, which includes J/ψ , $\psi(2S)$, higher excited states, and the hadronic continuum. Since the mass of state J/ψ is lower than that of state $\eta_c(2S)$, the transition $J/\psi \rightarrow \eta_c(2S)\gamma$ cannot occur. Therefore, the transition $\psi(2S) \rightarrow \eta_c(2S)\gamma$ is isolated,

$$\begin{aligned} \Pi_{\mu\nu}(Q, q) &= \frac{1}{m_{\psi(2S)}^2 - (q+Q)^2} \langle \eta_c(2S)(Q) | \bar{c}(0)\gamma_{\mu}c(0) | \psi(2S) \rangle \langle \psi(2S) | \bar{c}(0)\gamma_{\nu}c(0) | 0 \rangle \\ &+ \int_{s_0}^{\infty} ds \frac{\rho(Q^2, s)}{s - (Q+q)^2}, \end{aligned} \quad (16)$$

where $\rho(Q^2, s)$ is defined similarly to Eq. (3).

The decay matrix elements in Eq. (16) are parametrized as follows

$$\langle \eta_c(2S)(Q) | \bar{c}(0) \gamma_\mu c(0) | \psi(2S) \rangle = \varepsilon_{\mu\alpha\beta\gamma} Q^\beta q^\alpha \varepsilon^{\gamma*} F_{VP} \frac{2}{m_{\psi(2S)} + m_{\eta_c(2S)}}, \quad (17)$$

$$\langle \psi(2S) | \bar{c}(0) \gamma_\nu c(0) | 0 \rangle = m_{\psi(2S)} f_{\psi(2S)} \varepsilon_\nu, \quad (18)$$

here, $m_{\psi(2S)}$ is the mass of the $\psi(2S)$ meson, $m_{\eta_c(2S)}$ is the mass of the $\eta_c(2S)$ meson, $f_{\psi(2S)}$ is the decay constant, F_{VP} is the transition form factor. Through the substitution of Eq. (17) and (18) into Eq. (16), the phenomenological result is obtained

$$\begin{aligned} \Pi_{\mu\nu}(Q, q) &= \frac{1}{m_{\psi(2S)}^2 - (Q+q)^2} \frac{2\varepsilon_{\mu\alpha\beta\gamma} Q^\beta q^\alpha \varepsilon^{\gamma*} F_{VP} m_{\psi(2S)} f_{\psi(2S)} \varepsilon_\nu}{m_{\psi(2S)} + m_{\eta_c(2S)}} \\ &+ \int_{s_0}^{\infty} ds \frac{\frac{1}{\pi} \text{Im} \Pi(Q, q) \theta(s - s_0)}{s - (Q+q)^2}. \end{aligned} \quad (19)$$

On the other hand, the theoretical result for the correlation function is given by

$$\Pi_{\mu\nu}(Q, q) = 2\varepsilon_{\mu\alpha\nu\beta} f_{\eta_c(2S)} Q^\beta q^\alpha \int_0^1 du \frac{\phi_{\eta_c(2S)}(u)}{m_c^2 - (q+uQ)^2}. \quad (20)$$

where, $\phi_{\eta_c(2S)}(u)$ is defined analogously to Eq. (8). Matching the phenomenological side with the theoretical side and applying the Borel transformation to both sides, the analytical expression of the form factor for the process $\psi(2S) \rightarrow \eta_c(2S) \gamma$ is obtained

$$F_{VP} = \frac{m_{\psi(2S)} + m_{\eta_c(2S)}}{m_{\psi(2S)}} \frac{f_{\eta_c(2S)}}{f_{\psi(2S)}} \int_{\Delta}^1 du \frac{\phi_{\eta_c(2S)}(u)}{u} e^{-\frac{1}{uM^2} [m_c^2 + u(1-u)m_{\eta_c(2S)}^2 + (1-u)P'^2] + \frac{m_{\psi(2S)}^2}{M^2}}, \quad (21)$$

where $\Delta = \frac{1}{2m_{\eta_c(2S)}^2} \left[\sqrt{(s_0 - m_{\eta_c(2S)}^2 + P'^2)^2 + 4m_{\eta_c(2S)}^2(m_c^2 + P'^2)} - (s_0 - m_{\eta_c(2S)}^2 - q^2) \right]$.

C. Light-Cone Distribution Amplitudes

The LCDAs serve as essential non-perturbative input parameters. The typical functional forms of LCDAs employed in this work, along with the required parameters, are provided below.

For the process $K^{*-} \rightarrow K^- \gamma$, the LCDA of K^- meson is chosen as [58–60]

$$\phi_K(u, \mu) = 6u(1-u) \left[1 + \sum_{n=1}^4 a_n^K(\mu) C_n^{3/2}(2u-1) \right], \quad (22)$$

where, $C_n^{3/2}$ are the Gegenbauer polynomials, a_n^K are the corresponding Gegenbauer coefficients, and their numerical values are listed in Table I [61].

For the process $D^* \rightarrow D \gamma$, the LCDA of D meson is taken as [65]

$$\begin{aligned} \phi_D(u, \mu_0^2) &= \frac{A_{2;D} \sqrt{6u\bar{u}} Y}{8\pi^{3/2} f_D b_{2;D}} \left[1 + B_{2;D} C_2^{3/2}(2u-1) \right] \exp \left[-b_{2;D}^2 \frac{um_u^2 + \bar{u}m_c^2 - Y^2}{u\bar{u}} \right] \\ &\times \left[\text{Erf} \left(\frac{b_{2;D} \sqrt{\mu_0^2 + Y^2}}{\sqrt{u\bar{u}}} \right) - \text{Erf} \left(\frac{b_{2;D} Y}{\sqrt{u\bar{u}}} \right) \right], \end{aligned} \quad (23)$$

TABLE I: Gegenbauer coefficients of K^- meson at the scale $\mu = 1$ GeV, obtained from QCDSR, LQCD and LFQM methods.

	a_1^K	a_2^K
Fit	0.331 ± 0.082	0.28 ± 0.10
QCDSR [62]	0.06 ± 0.03	0.25 ± 0.15
LQCD [63]	0.053 ± 0.003	0.09 ± 0.02
LFQM [64]	0.09 ± 0.13	0.03 ± 0.03

where $Y = um_d + \bar{u}m_c$. Moreover, at the energy scale $\mu_0 = 2$ GeV, the parameters are set to $B_{2;D} = 0.2397, A_{2;D} = 9.7736, b_{2;D} = -0.2244$ [65].

For the decays $B^* \rightarrow B\gamma, B_s^* \rightarrow B_s\gamma, \text{ and } D_s^{*+} \rightarrow D_s^+\gamma$, the LCDAs of the heavy-light mesons B^*, B_s^* , and D_s^{*+} are parameterized exponentially as [66]

$$\phi_H(u, \mu) = N(\alpha, \beta) 4u\bar{u}e^{4\alpha u\bar{u} + \beta(u-\bar{u})}, \quad (24)$$

where

$$N(\alpha, \beta) = 16\alpha^{5/2} [4\sqrt{\alpha}(\beta \sinh(\beta) + 2\alpha \cosh(\beta)) + e^{\alpha + \frac{\beta^2}{4\alpha}}(-2\alpha + 4\alpha^2 - \beta^2) \times \left\{ \text{Erf}\left(\frac{\alpha - \beta}{2\sqrt{\alpha}}\right) + \text{Erf}\left(\frac{\alpha + \beta}{2\sqrt{\alpha}}\right) \right\}]^{-1}. \quad (25)$$

The parameters α and β are presented in Table II, and Erf here denotes the error function.

TABLE II: The parameters α and β in the LCDAs of B^*, D_s^{*+} and B_s^* mesons at the scale $\mu = 2$ GeV [66].

	α	β
$B^* \rightarrow B\gamma$	0.360 ± 0.017	5.706 ± 0.225
$D_s^{*+} \rightarrow D_s^+\gamma$	0.712 ± 0.157	0.929 ± 0.082
$B_s^* \rightarrow B_s\gamma$	1.205 ± 0.526	6.109 ± 0.594

For the process $\psi(2S) \rightarrow \eta_c(2S)\gamma$, the BHL approach [57, 67, 68] is used to define the LCDA of $\eta_c(2S)$ meson,

$$\phi_{\eta_c(2S)}(u, \mu_0) = \frac{2\sqrt{6}}{f_{\eta_c(2S)}} \int_{|\vec{k}_\perp|^2 < \mu_0^2} \frac{d^2\vec{k}_\perp}{16\pi^3} \Psi_{\eta_c(2S)}(u, \vec{k}_\perp), \quad (26)$$

$$\Psi_{\eta_c(2S)}^{\lambda_1\lambda_2}(u, \vec{k}_\perp) = \phi_{BHL}(u, \vec{k}_\perp) \chi^{\lambda_1\lambda_2}(u, \vec{k}_\perp) = A e^{-b^2 \frac{\vec{k}_\perp^2 + m_c^2}{u(1-u)}} \chi^{\lambda_1\lambda_2}(u, \vec{k}_\perp), \quad (27)$$

where, $\Psi_{\eta_c(2S)}^{\lambda_1\lambda_2}(u, \vec{k}_\perp)$ is the wave function of $\eta_c(2S)$ meson, and $\chi^{\lambda_1\lambda_2}(u, \vec{k}_\perp)$ [69–71] is the spin wave function, as presented in Table III. The parameters A and b^2 are determined by the following two constraints

$$\begin{aligned} \frac{2\sqrt{6}}{f_{\eta_c(2S)}} \int_0^1 dx \int_{|\vec{k}_\perp|^2 < \mu_0^2} \frac{d^2\vec{k}_\perp}{16\pi^3} \sum_{\lambda_1\lambda_2} \Psi_{\eta_c(2S)}^{\lambda_1\lambda_2}(u_i, \vec{k}_\perp) &= 1, \\ \int_0^1 dx \int \frac{d^2\vec{k}_\perp}{16\pi^3} |\phi_{BHL}(u, \vec{k}_\perp)|^2 &= P_{\eta_c(2S)}. \end{aligned} \quad (28)$$

The first equation in (28) is the normalization condition, and the second equation corresponds to the probability normalization condition, where $P_{\eta_c(2S)}$ denotes the proportion of the Fock state. Here, we select the leading order in the Fock state expansion with $P_{\eta_c(2S)} = 0.5$, and assume that the initial scale of the distribution amplitude of $\eta_c(2S)$ meson is $\mu_0 = m_c^*$. Using these inputs, the two undetermined parameters are obtained as $A = 21.7713 \text{ GeV}^{-1}$ and $b^2 = 0.06787 \text{ GeV}^{-2}$.

TABLE III: The spin wave function for $\eta_c(2S)$. Here, $m_c^* = 1.8 \text{ GeV}$ [72] is the constituent quark mass of the c-quark, and λ_1 and λ_2 denote the helicities of the c-quark and the anti-c-quark, respectively.

	$\uparrow\uparrow$	$\uparrow\downarrow$	$\downarrow\uparrow$	$\downarrow\downarrow$
$\chi^{\lambda_1\lambda_2}(u, \vec{k}_\perp)$	$-\frac{k_x - ik_y}{\sqrt{2(m_c^{*2} + k_\perp^2)}}$	$\frac{m_c^*}{\sqrt{2(m_c^{*2} + k_\perp^2)}}$	$-\frac{m_c^*}{\sqrt{2(m_c^{*2} + k_\perp^2)}}$	$-\frac{k_x + ik_y}{\sqrt{2(m_c^{*2} + k_\perp^2)}}$

D. Decay Width

Once the form factors are determined, the M1 radiative decay widths for the processes $K^{*-} \rightarrow K^- \gamma$, $D^* \rightarrow D \gamma$, $B^* \rightarrow B \gamma$, $D_s^{*+} \rightarrow D_s^+ \gamma$, and $B_s^* \rightarrow B_s \gamma$, can be obtained [73]

$$\Gamma = \frac{\alpha}{3} g_{VP\gamma}^2 k_\gamma^3, \quad (29)$$

where α is the fine structure constant, $k_\gamma = (M_V^2 - M_P^2)/2M_V$, and the coupling constant $g_{VP\gamma}$ for a real photon is equal to the form factor $F_{VP}(q^2)$ in the limit $q^2 \rightarrow 0$.

For the decay $\psi(2S) \rightarrow \eta_c(2S)\gamma$, considering the superior symmetry properties of $c\bar{c}$ states compared to those in heavy-light mesonic systems, the decay width formula can be further simplified to [55]

$$\Gamma = \alpha \frac{(m_i^2 - m_f^2)^3}{(2m_i)^3 (m_i + m_f)^2} \frac{64}{27} |F_{VP}|^2, \quad (30)$$

here, m_i and m_f are the masses of $\psi(2S)$ and $\eta_c(2S)$, respectively.

III. NUMERICAL RESULTS AND DISCUSSION

A. Input Parameters

In the preceding sections, analytic expressions for the form factors and decay widths of the six decay processes have been derived. In the subsequent discussion, numerical results will be

provided and compared with experimental measurements along with predictions from other theoretical approaches.

The input parameters consist of two parts: some are taken from the PDG [6] (e.g., quark masses), compiled in Table IV and others are required by the LCSR analysis, including the thresholds and the Borel parameters.

TABLE IV: Parameters required for all processes include quark masses, decay constants, and meson masses.

Processes	Quark masses(GeV) [6]	Decay constants(GeV) [59, 74, 75]	Meson masses(GeV) [6]
$K^{*-} \rightarrow K^- \gamma$	$m_s = 0.0935$	$f_{K^-} = 0.156, f_{K^{*-}} = 0.226$	$m_{K^-} = 0.4936, m_{K^{*-}} = 0.890$
$D^* \rightarrow D \gamma$	$m_c = 1.273, m_u = 0.00216$	$f_D = 0.206, f_D^* = 0.265$	$m_D = 1.864, m_{D^*} = 2.007$
$B^* \rightarrow B \gamma$	$m_b = 4.183$	$f_B = 0.188, f_B^* = 0.215$	$m_B = 5.279, m_{B^*} = 5.324$
$D_s^{*+} \rightarrow D_s^+ \gamma$	$m_c = 1.273$	$f_{D_s^+} = 0.219, f_{D_s^{*+}} = 0.375$	$m_{D_s^+} = 1.968, m_{D_s^{*+}} = 2.106$
$B_s^* \rightarrow B_s \gamma$	$m_b = 4.183$	$f_{B_s} = 0.235, f_{B_s^*} = 0.256$	$m_{B_s} = 5.366, m_{B_s^*} = 5.415$
$\psi(2S) \rightarrow \eta_c(2S) \gamma$	$m_c = 1.273$	$f_{\eta_c(2S)} = 0.318, f_{\psi(2S)} = 0.294$	$m_{\eta_c(2S)} = 3.637, m_{\psi(2S)} = 3.686$

Within the LCSR framework, the threshold and the Borel parameter are crucial input parameters. As a common practice, the threshold is taken to be the squared mass of the first excited state meson, although its precise value depends on the specific decay channel and must be fixed separately. For the decay $K^{*-} \rightarrow K^- \gamma$, the first excited state of the K^* meson, $K^*(1410)$, has a mass of 1.414 GeV, so the threshold s_0 is approximately 1.9 GeV^2 . The Borel parameter is typically determined by imposing two criteria:

1. The combined contribution from higher resonances and the continuum is less than 30%;
2. The physical observables exhibit only mild dependence on the Borel parameter.

B. Transition Form Factors

Based on the criteria and constraints established above, the dependence of the form factors on the threshold s_0 and Borel parameter M^2 is discussed as follows.

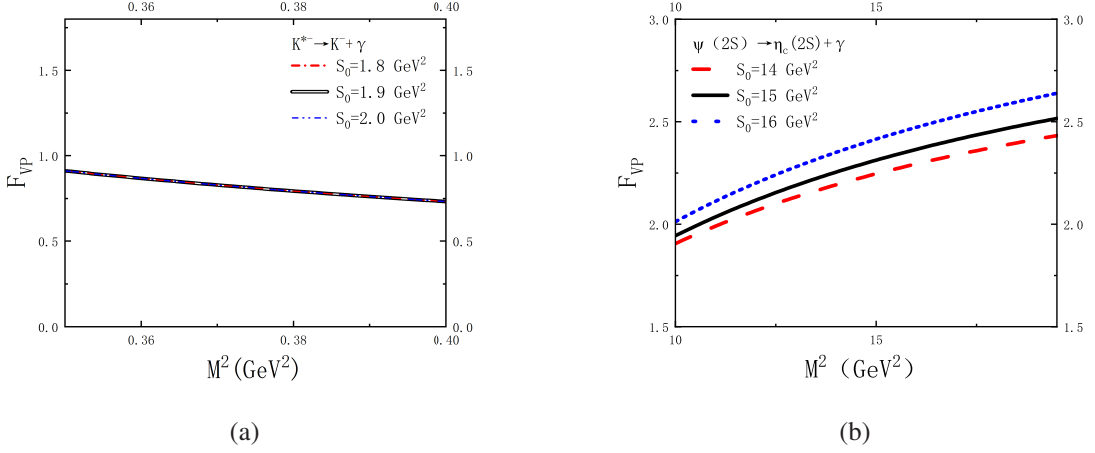


FIG. 1: The dependence of the form factors for $K^{*-} \rightarrow K^- \gamma$ and $\psi(2S) \rightarrow \eta_c(2S) \gamma$ processes on the threshold s_0 and Borel parameter M^2 .

The form factor for $K^{*-} \rightarrow K^- \gamma$ process is shown in Fig. 1(a). The threshold parameter is chosen as $s_0 \approx 1.9$ GeV². As shown in Fig. 1(a), our results are highly stable under variations of the thresholds. In contrast, they exhibit a moderate dependence on the Borel parameter.

Building on the transition form factors we have obtained for ground state vector mesons [56], we extend our calculation to excited state M1 radiative decay $\psi(2S) \rightarrow \eta_c(2S) \gamma$. As shown in Fig. 1(b), the results of the form factor exhibits a certain sensitivity to the Borel parameter, while maintaining only weak dependence on the thresholds.

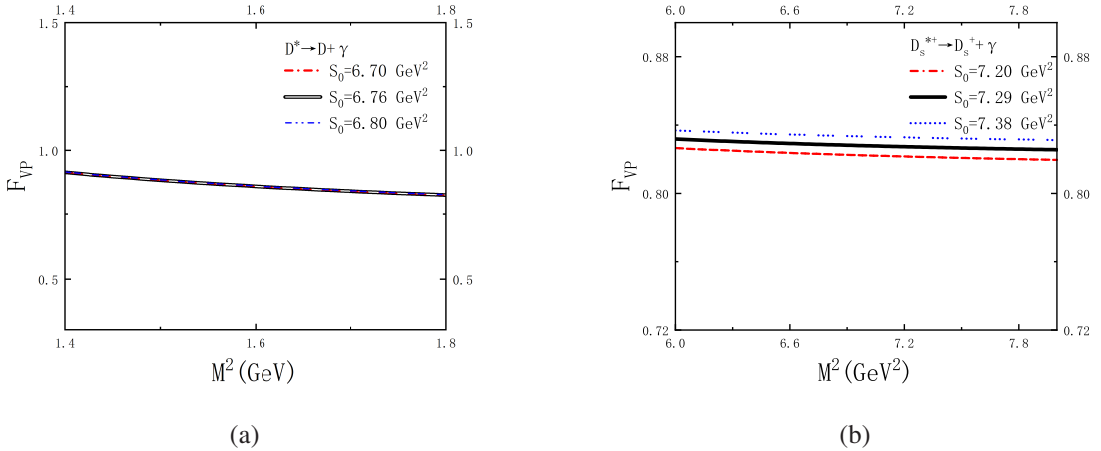


FIG. 2: The dependence of the form factors for $D^* \rightarrow D \gamma$ and $D_s^{*+} \rightarrow D_s^+ \gamma$ processes on the threshold s_0 and Borel parameter M^2 .

Experimental data on the $D^* \rightarrow D \gamma$ transition remain imprecise at present. In Fig. 2(a), we choose the threshold near the square of the mass of $D_1^{*0}(2600)$ [6]. Within the LCSR framework, the form factor is remarkably stable against variations of the thresholds. By contrast, the results exhibit a certain dependence on the Borel parameter.

Similar to the $D^* \rightarrow D \gamma$ process, we select the threshold near the square of the $D_{s1}^*(2700)^\pm$ meson mass [6], $s_0 = 7.29$ GeV². As shown in Fig. 2(b), the transition form factor for $D_s^{*+} \rightarrow D_s^+ \gamma$

exhibits excellent stability under variations of the thresholds, and the results of the form factor display only a mild dependence on the Borel parameter.

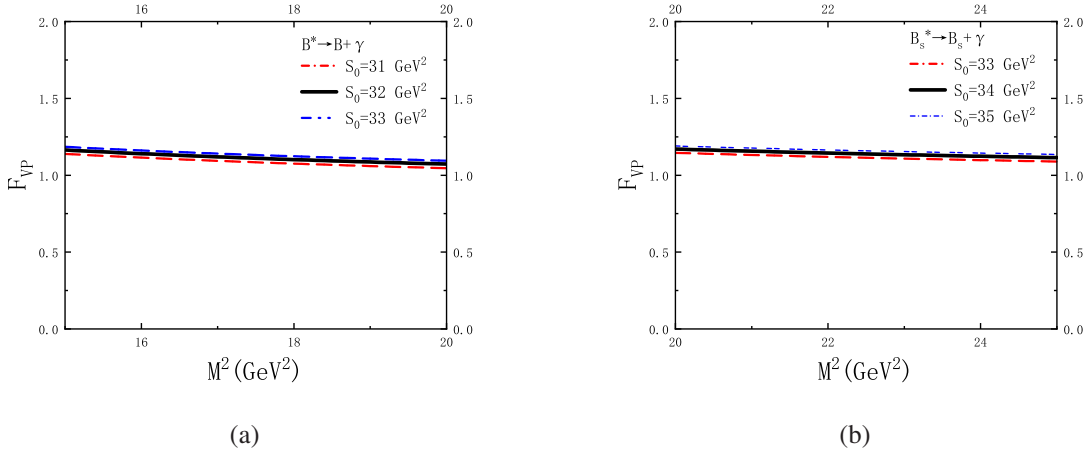


FIG. 3: The dependence of the form factors for $B^* \rightarrow B\gamma$ and $B_s^* \rightarrow B_s\gamma$ processes on the threshold s_0 and Borel parameter M^2 .

In experiments, the total decay widths of the B^* and B_s^* mesons and the branching fractions for their M1 radiative decays have not yet been precisely determined. As shown in Fig. 3, the transition form factors for the $B^* \rightarrow B\gamma$ and $B_s^* \rightarrow B_s\gamma$ processes exhibit a high degree of stability under variations of the Borel parameter, with almost negligible impact. Further, the form factors display weak dependence on the threshold. This minor variation stems primarily from the insufficient knowledge of the first excited state in these decay channels, which directly affects the choice of the threshold parameter and constitute the main source of uncertainty.

C. Numerical Results for the Form Factors F_{VP}

Based on the above sensitivity analysis, we present the numerical values of the transition form factors at fixed Borel parameters and thresholds in Table V at the limit $q^2 = 0$. In this work, with the parameters choice $s_0 = 1.9 \text{ GeV}^2$ and $M^2 = 0.38 \text{ GeV}^2$, we present numerical results for the $K^{*-} \rightarrow K^-\gamma$ transition form factor. The parameters adopted for the other channels are: $D^* \rightarrow D\gamma$ ($s_0 = 6.76 \text{ GeV}^2$, $M^2 = 1.60 \text{ GeV}^2$), $B^* \rightarrow B\gamma$ ($s_0 = 32 \text{ GeV}^2$, $M^2 = 18 \text{ GeV}^2$), $D_s^{*+} \rightarrow D_s^+\gamma$ ($s_0 = 7.29 \text{ GeV}^2$, $M^2 = 7 \text{ GeV}^2$), $B_s^* \rightarrow B_s\gamma$ ($s_0 = 34 \text{ GeV}^2$, $M^2 = 23 \text{ GeV}^2$), and $\psi(2S) \rightarrow \eta_c(2S)\gamma$ ($s_0 = 16 \text{ GeV}^2$, $M^2 = 15 \text{ GeV}^2$).

TABLE V: Numerical results of the form factors $F_{VP}(q^2)$ at the limit $q^2 \rightarrow 0$.

	$K^{*-} \rightarrow K^-\gamma$	$D^* \rightarrow D\gamma$	$D_s^{*+} \rightarrow D_s^+\gamma$	$B^* \rightarrow B\gamma$	$B_s^* \rightarrow B_s\gamma$	$\psi(2S) \rightarrow \eta_c(2S)\gamma$
$F_{VP}(q^2 = 0)$	0.835	0.861	0.827	1.101	1.132	2.356

The LCSR method is equally applicable in the nonzero region $0 \leq q^2 \leq (M_V - M_P)^2$. For the M1 radiative transitions, this q^2 window is intrinsically very narrow. As a consequence, the

dependence of form factors on the q^2 in this interval is very mild and numerically essentially coincides with its value at $q^2 = 0$. Given the negligible q^2 dependence, we do not explore this further.

D. Numerical Results for the Decay Widths

In the aforementioned section, we discussed the transition form factors, an important nonperturbative physical parameter. In this section, we will present the results of the M1 radiative decay widths using the transition form factors. We visually illustrate the dependence of M1 radiative decay widths on the thresholds s_0 and Borel parameters M^2 .

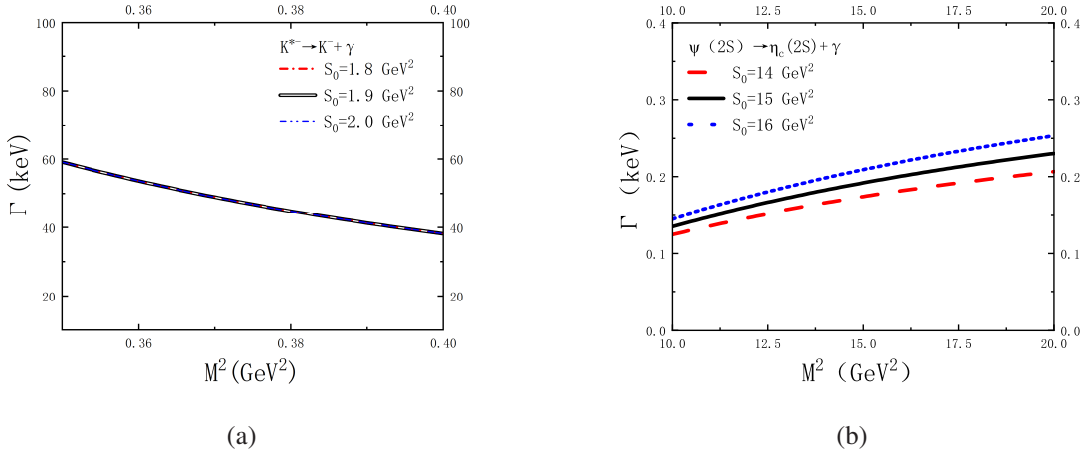


FIG. 4: The dependence of the decay widths for $K^{*-} \rightarrow K^- \gamma$ and $\psi(2S) \rightarrow \eta_c(2S) \gamma$ processes on the threshold s_0 and Borel parameter M^2 .

The Fig. 4 shows the dependence of the decay widths for the processes $K^{*-} \rightarrow K^- \gamma$ and $\psi(2S) \rightarrow \eta_c(2S) \gamma$ on the thresholds s_0 and the Borel parameters M^2 . It is evident from the figure that the decay widths are highly stable under variation of the thresholds, whereas they exhibit certain degree of sensitivity on the Borel parameter. The Appendix presents plots illustrating the continuous variation of selected decay widths with the thresholds s_0 and the Borel parameters M^2 ; further details are provided in Appendix A.

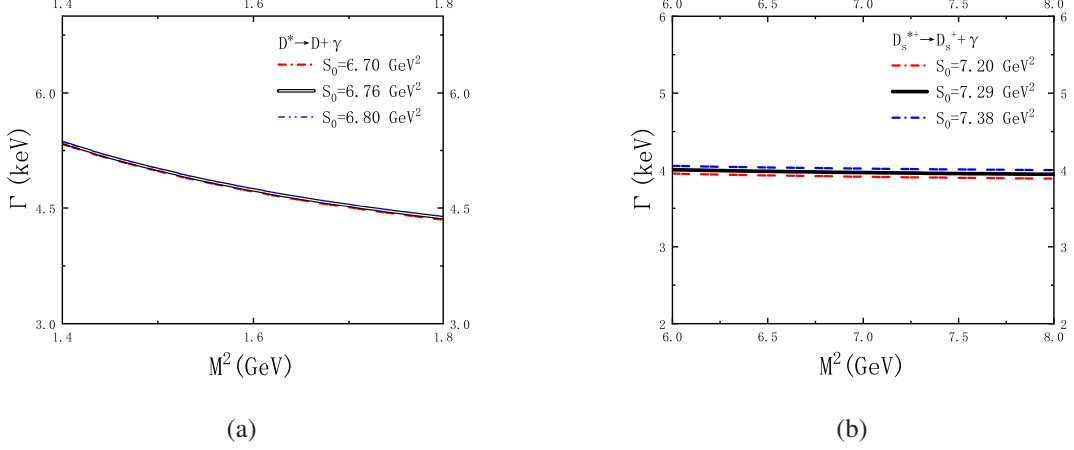


FIG. 5: The dependence of the decay widths for $D^* \rightarrow D\gamma$ and $D_s^{*+} \rightarrow D_s^+\gamma$ processes on the threshold s_0 and Borel parameter M^2 .

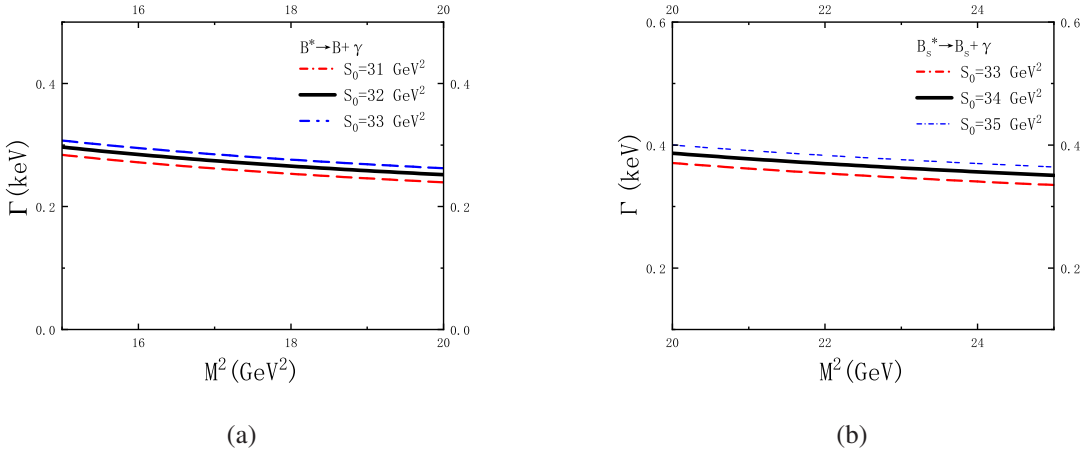


FIG. 6: The dependence of the decay widths for $B^* \rightarrow B\gamma$ and $B_s^{*+} \rightarrow B_s^+\gamma$ processes on the threshold s_0 and Borel parameter M^2 .

The M1 radiative decay width for the $K^{*-} \rightarrow K^-\gamma$ process, as quoted in the Particle Data Group (PDG) review, is 50.37 keV [6]. The result obtained in this work using the LCSR method is 51.1 keV, with a relative deviation of approximately 1.5% compared to the value shown in the PDG. For the excited state $\psi(2S) \rightarrow \eta_c(2S)\gamma$ process, the calculated result in this work is 51.1 keV, and the relative deviation from the experimental value of 0.15 keV [15] is approximately 33%. This discrepancy could be attributed to several factors, including the neglect of higher-order corrections, the sensitivity of the excited-state calculation to the LCSR parameters and the challenges in modeling the LCDA for the $\eta_c(2S)$ meson.

Theoretical predictions for the M1 radiative decay widths of four processes ($D^* \rightarrow D\gamma$, $B^* \rightarrow B\gamma$, $D_s^{*+} \rightarrow D_s^+\gamma$ and $B_s^{*+} \rightarrow B_s^+\gamma$) are presented in Figs. 5 and 6. In Table VI, we compare our results of the decay widths with those obtained from experiments and from other theoretical approaches.

TABLE VI: The M1 radiative decay widths for all processes are presented (in units of keV). The first row shows our theoretical predictions, and the second row displays the corresponding experimental measurements. Furthermore, we systematically compare our theoretical results with predictions from several models, including QCD sum rules (QCDSR), vector confining potentials (VCP), relativistic quark model(RQM), non-relativistic potential model(PM), effective mass scheme(EMS), scalar confining potentials (SCP), light-front quark model (LFQM), and nonrelativistic quark model (NRQM).

	$K^{*-} \rightarrow K^- \gamma$	$D^{*+} \rightarrow D \gamma$	$D_s^{*+} \rightarrow D_s^+ \gamma$	$B^* \rightarrow B \gamma$	$B_s^* \rightarrow B_s \gamma$	$\psi(2S) \rightarrow \eta_c(2S) \gamma$
This work	$51.1^{+7.8}_{-12.9}$	$4.73^{+0.62}_{-0.35}$	$3.96^{+0.04}_{-0.02}$	$0.26^{+0.03}_{-0.01}$	$0.36^{+0.03}_{-0.01}$	$0.2^{+0.02}_{-0.07}$
EXP [6, 15]	50.37	-	-	-	-	0.15
VCP [76]	-	14.3	-	0.087	0.064	-
SCP [76]	-	17.4	-	0.101	0.074	-
RIQ [77]	-	26.5	0.213	0.181	0.119	-
LFQM [20, 21, 73]	79.5	20.0 ± 0.3	0.17	0.13 ± 0.01	0.068 ± 0.017	0.11
NRQM [23, 76]	-	37	-	0.27	0.132	0.21
LCSR [78]	-	14.4	-	0.16	-	-
QCDSR [26]	-	12.9 ± 2	-	0.13 ± 0.03	0.22 ± 0.04	-
HQET [79]	-	16.0 ± 7.5	-	0.075 ± 0.027	-	-
PM [80, 81]	104.46	35.506	0.284	-	-	-
EMS [80]	62.988	11.731	0.130	-	-	-
RQM [82]	-	97	-	-	-	-

We find that the decay widths generally decrease from the strange (K^*) to the charm (D^*) and bottom (B^*) sectors, reflecting the phase-space suppression for heavier mesons. However, the widths for strange-containing mesons (D_s^{*+}, B_s^*) are notably enhanced compared to their non-strange counterparts (D^*, B^*). This behavior, which may appear as an anomaly, is in fact physically expected and can be attributed to the explicit breaking of flavor symmetry by the strange quark, an effect consistent with expectations from heavy-quark effective theory [83, 84].

E. Linear Relationship

An intriguing systematic behavior emerges from our analysis of the ground-state $V \rightarrow P \gamma$ decays. We find that the decay widths exhibit a universal scaling relation when plotted against a specific kinematic function. Motivated by the two-body decay dynamics and the role of decay constant, we define the function $A(x)$ as

$$A(x) = \left(\frac{f_f}{f_i} \frac{1}{(m_f + m_i)^2} \right) k_\gamma^3 (F_{VP})^x, \quad (31)$$

where, x is a free power to be determined, f_i and f_f are the decay constants of the initial and final states, m_i and m_f are the masses corresponding to the initial and final state mesons and k_γ is the photon momentum.

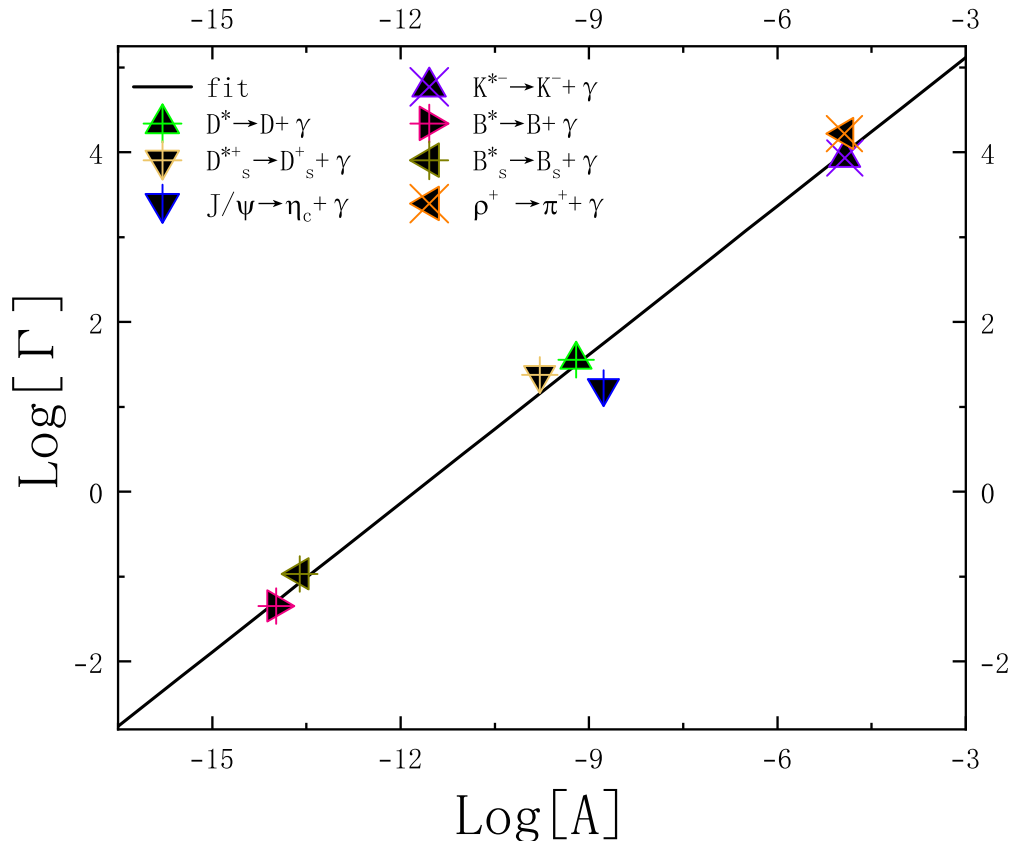


FIG. 7: Linear dependence of the decay width on the function A in the logarithmic coordinate system.

Remarkably, when plotting the decay width Γ against $A(x)$ in the logarithmic coordinate system, all data points for the ground-state transitions align along a straight line for an optimal power of $x \approx 2.1$, as shown in Fig. 7. This observed linear dependence, $\log(\Gamma) \propto \log(A(2.1))$ suggests a universal pattern governing these M1 radiative decays. The fact that the optimal power is not exactly 2 (as a naive leading-order analysis might suggest in Eq. (30)) indicates the significance of contributions beyond the leading order, such as higher-order perturbative QCD corrections and higher-twist effects. Additionally, we have also collected the meson masses, decay constants, radiative decay widths, and transition form factors for the processes $J/\psi \rightarrow \eta_c \gamma$ and $\rho^+ \rightarrow \pi^+ \gamma$ [6, 35, 85], also fall neatly on the same fitted line. This observation could provide a fresh, unifying perspective on the systematics of radiative decays.

IV. SUMMARY

In this work, we study the magnetic dipole (M1) radiative decays of vector mesons within the framework of LCSR. Firmly grounded in the first principles of QCD, this method provides a computationally efficient tool for determining transition form factors with minimal model dependence. We apply it to a set of vector mesons systems spanning the strange, charm, and bottom sectors

(K^* , B^* , B_s^* , D^* , D_s^{*+}) and extend the formalism to the radiative transition between excited charmonium states, $\psi(2S) \rightarrow \eta_c(2S)\gamma$. The core of this work lies in the computation of the transition form factors for these decay channels, from which the corresponding M1 radiative decay widths are derived.

Our numerical results of the decay widths are consistent with existing experimental data. For the ground state vector meson channel $K^{*-} \rightarrow K^-\gamma$, we predict $\Gamma(K^{*-} \rightarrow K^-\gamma) = 51.1_{-12.9}^{+7.8}$ keV, in excellent agreement with the measured value of 50.3 keV [6]. For the charmonium transition $\psi(2S) \rightarrow \eta_c(2S)\gamma$, we obtain $\Gamma(\psi(2S) \rightarrow \eta_c(2S)\gamma) = 0.20_{-0.07}^{+0.02}$ keV, which is consistent with the experimental value of 0.15 keV [15] within uncertainties. For channels not yet measured experimentally, we provide the following theoretical predictions: $\Gamma(D^* \rightarrow D\gamma) = 4.73_{-0.35}^{+0.62}$ keV, $\Gamma(D_s^{*+} \rightarrow D_s^+\gamma) = 3.96_{-0.02}^{+0.04}$ keV, $\Gamma(B^* \rightarrow B\gamma) = 0.26_{-0.01}^{+0.03}$ keV, and $\Gamma(B_s^* \rightarrow B_s\gamma) = 0.36_{-0.01}^{+0.03}$ keV. A comprehensive comparison with a range of other theoretical approaches including quark models, lattice QCD, and alternative QCD sum rule calculations shows broad consistency, thereby further reinforcing the credibility of our predictions.

While this work provides individual predictions for decay widths, it also reveals a linear behavior governing these transition processes. For the vector mesons (K^* , D^* , B^*), the decay width exhibits a monotonic decrease with increasing vector meson mass. A distinct flavor dependent effect is observed: the decay widths of heavy mesons containing strange quarks (D_s^{*+} , B_s^*) exhibit a discernible deviation from the overall trend. Moreover, when analyzed in logarithmic coordinates, the widths for all channels including charmonium systems reveal a striking linear scaling relation with an appropriate kinematic function derived from two-body decay dynamics. This finding suggests a potential universality underlying M1 transitions. Deviations from the fitted linear relation are primarily attributed to the leading order truncation in our computational framework, particularly the omission of higher order perturbative QCD corrections and higher twist contributions.

In summary, the light-cone sum rules framework has been employed to compute radiative partial widths for a representative set of vector meson decays, yielding results consistent with experimental data while providing valuable physical insights. The observed linear behavior offers a new perspective on the systematics of hadronic radiative transitions. In subsequent work, we will focus on incorporating higher order corrections and related factors to enhance the precision of our results and reduce theoretical uncertainties. Furthermore, we plan to include processes with different spin configurations, thereby enabling more rigorous tests of the linear behavior observed in the present study. On the experimental front, high precision measurements of radiative widths for bottom and charmed mesons from ongoing and future facilities, particularly Belle II and LHCb, are anticipated to provide critical tests of these theoretical predictions and further constrain nonperturbative QCD models. Such coordinated efforts will undoubtedly advance our fundamental understanding of strong interaction dynamics in the nonperturbative regime.

ACKNOWLEDGMENTS

We would like to thank Wen-Nian Liu, Chen Wang, and Wen-Xuan Zhang for stimulating discussions. This work was supported by the China Scholarship Council (Grant No. 202510530001).

Appendix A

In Section III, we present a detailed discussion of the choice of the Borel parameter M^2 and the continuum threshold s_0 , and we provide a quantitative assessment of how the transition form factors and the M1 radiative decay widths depend on these inputs. The figures in Section III illustrate the impact of continuous variation of the Borel parameter. For the threshold parameter, we analyze several representative values. For completeness and generality, Appendix A provides a detailed account of the dependence of the transition form factors and the decay widths on the parameters M^2 and s_0 for all processes considered in this work.

For the process $K^* \rightarrow K^+ \gamma$,

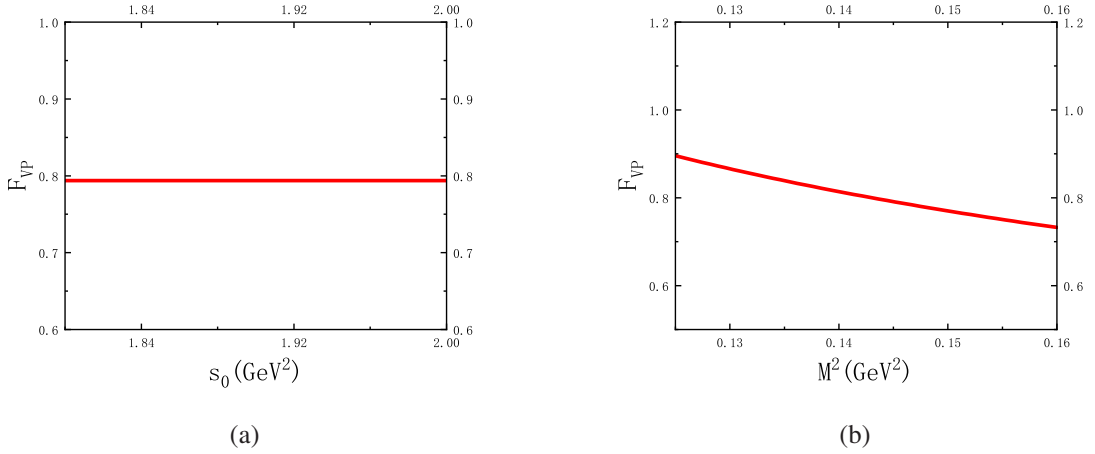


FIG. 8: The dependence of the form factors for $K^{*-} \rightarrow K^- \gamma$ process on the threshold s_0 and Borel parameter M^2 .

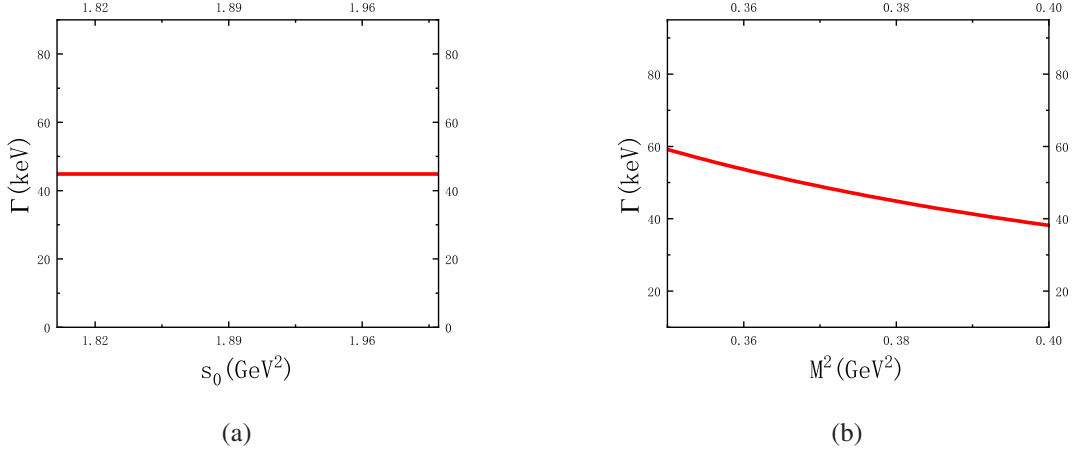


FIG. 9: The dependence of the decay widths for $K^{*-} \rightarrow K^- \gamma$ process on the threshold s_0 and Borel parameter M^2 .

For the process $D^* \rightarrow D \gamma$,

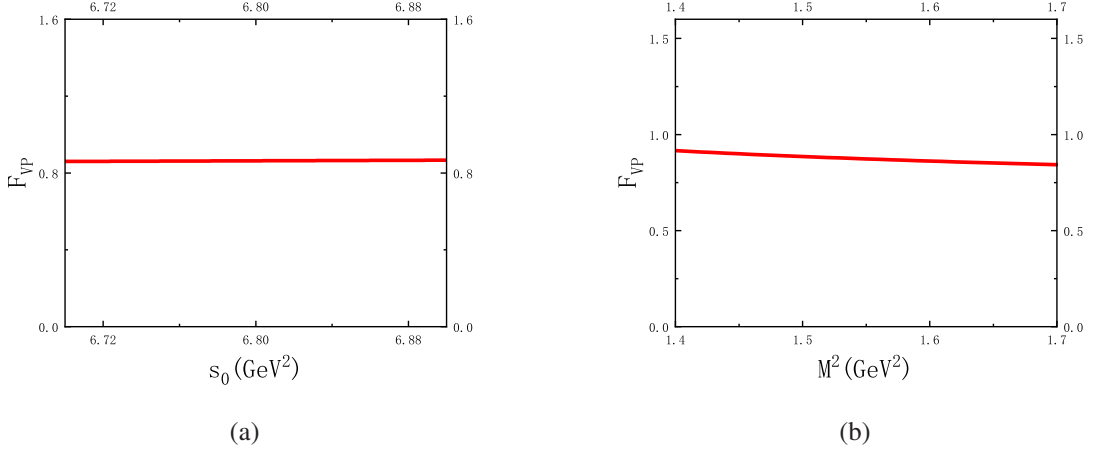


FIG. 10: The dependence of the form factors for $D^* \rightarrow D\gamma$ process on the threshold s_0 and Borel parameter M^2 .

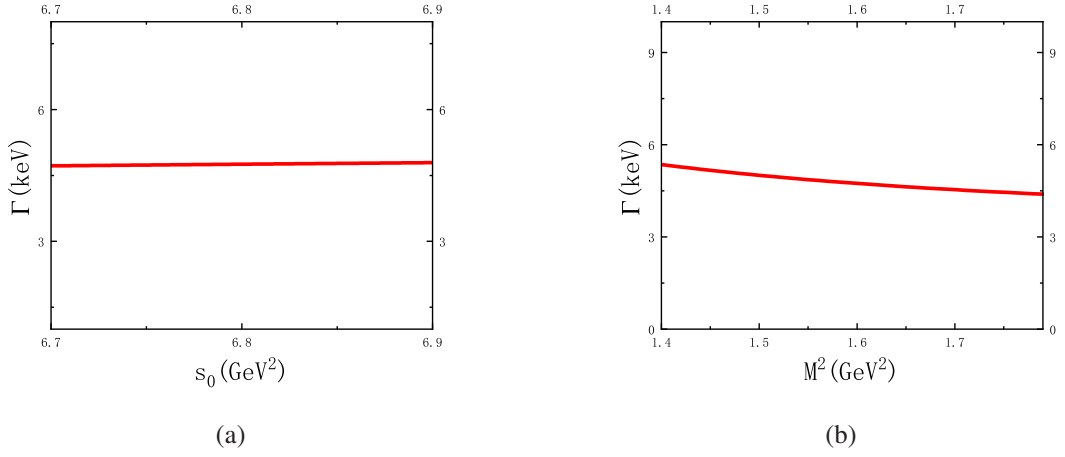


FIG. 11: The dependence of the decay widths for $D^* \rightarrow D\gamma$ process on the threshold s_0 and Borel parameter M^2 .

For the process $B^* \rightarrow B\gamma$,

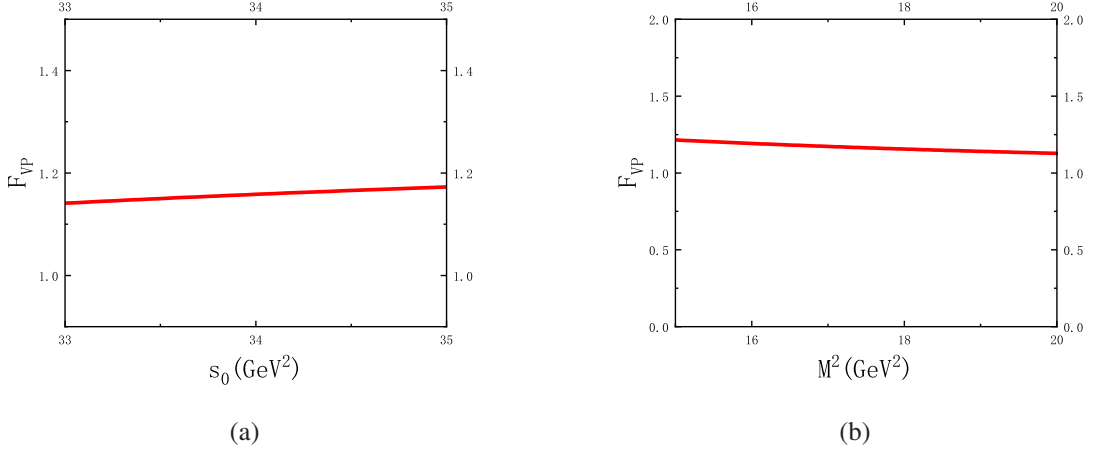


FIG. 12: The dependence of the form factors for $B^* \rightarrow B\gamma$ process on the threshold s_0 and Borel parameter M^2 .

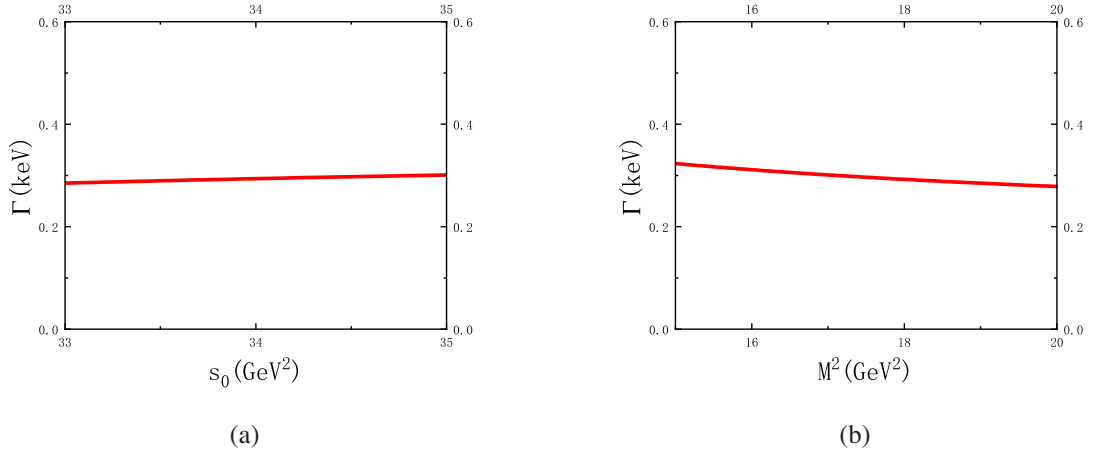


FIG. 13: The dependence of the decay widths for $B^* \rightarrow B\gamma$ process on the threshold s_0 and Borel parameter M^2 .

For the process $D_s^{*+} \rightarrow D_s^+\gamma$,

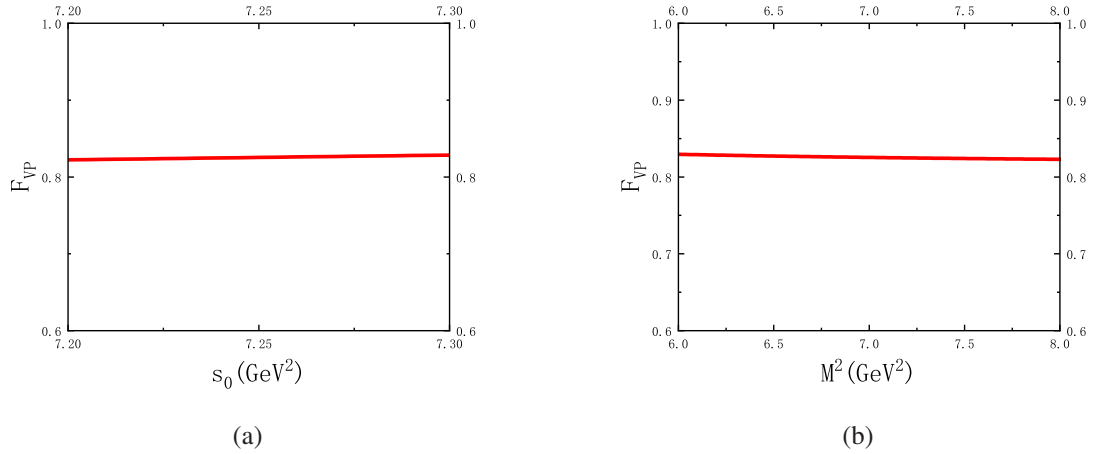


FIG. 14: The dependence of the form factors for $D_s^{*+} \rightarrow D_s^+ \gamma$ process on the threshold s_0 and Borel parameter M^2 .

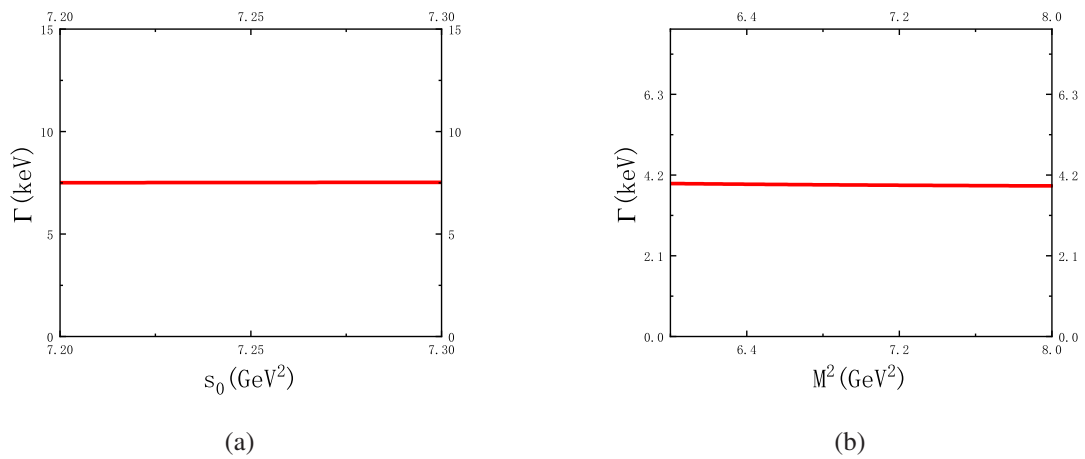


FIG. 15: The dependence of the decay widths for $D_s^{*+} \rightarrow D_s^+ \gamma$ process on the threshold s_0 and Borel parameter M^2 .

For the process $B_s^* \rightarrow B_s \gamma$,

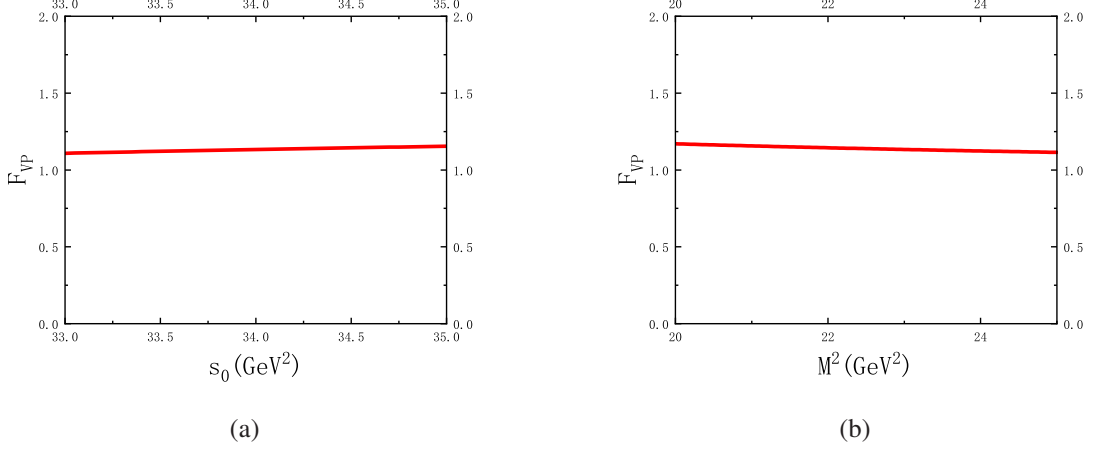


FIG. 16: The dependence of the form factors for $B_s^* \rightarrow B_s \gamma$ process on the threshold s_0 and Borel parameter M^2 .

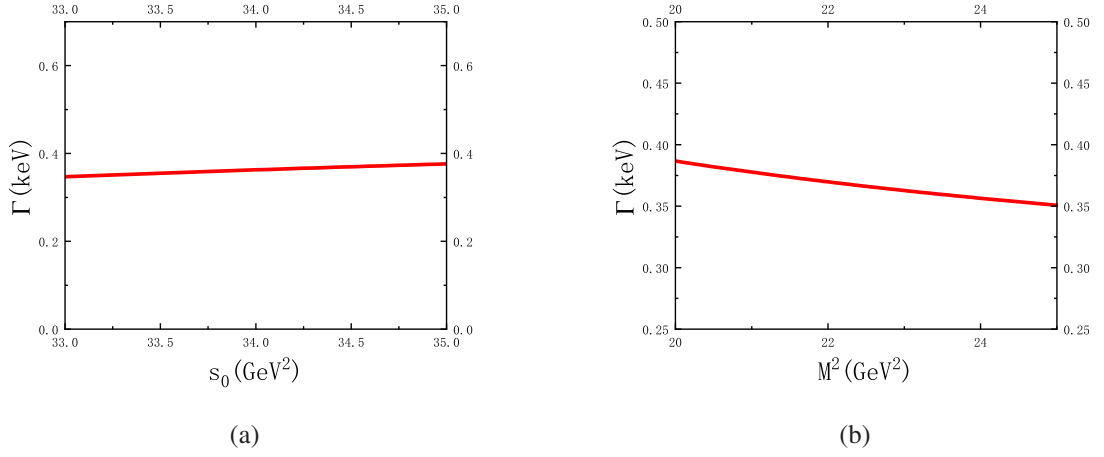


FIG. 17: The dependence of the decay widths for $B_s^* \rightarrow B_s \gamma$ process on the threshold s_0 and Borel parameter M^2 .

For the process $\psi(2S) \rightarrow \eta_c(2S) \gamma$,

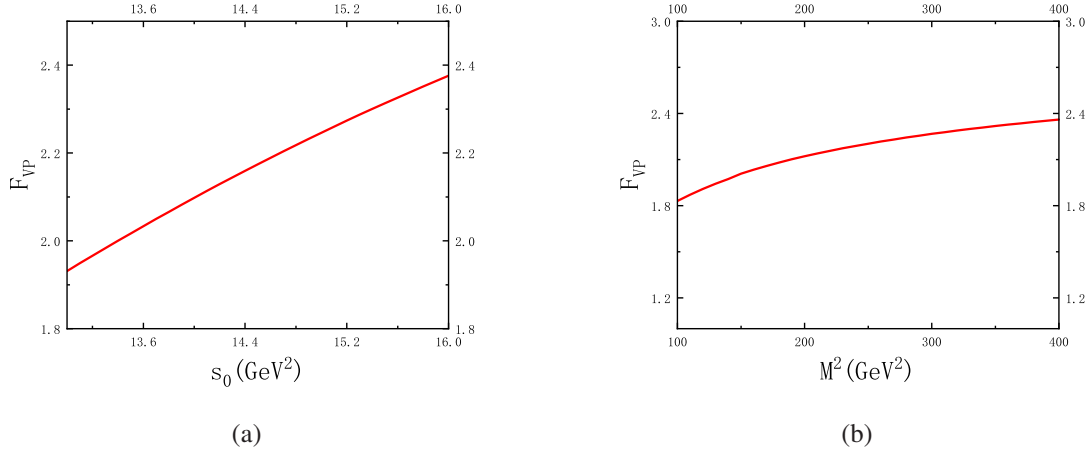


FIG. 18: The dependence of the form factors for $\psi(2S) \rightarrow \eta_c(2S)\gamma$ process on the threshold s_0 and Borel parameter M^2 .

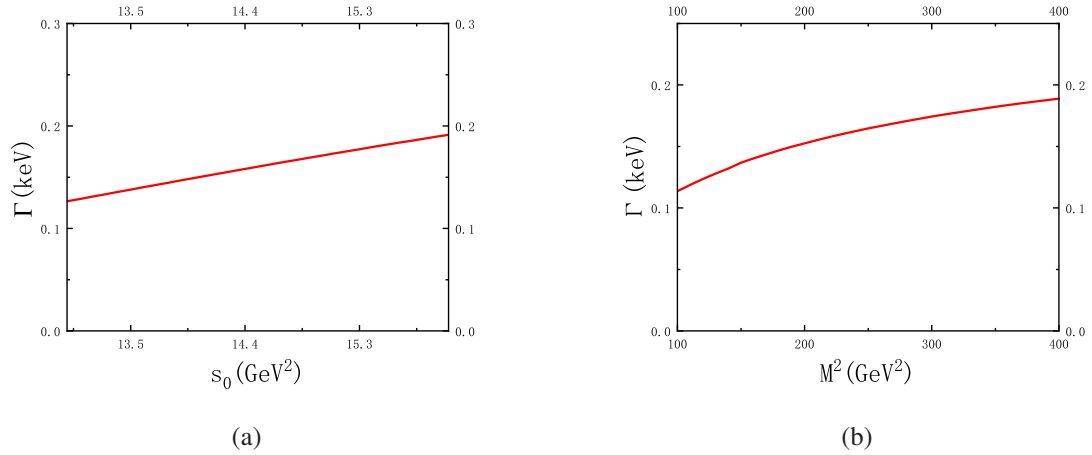


FIG. 19: The dependence of the decay widths for $\psi(2S) \rightarrow \eta_c(2S)\gamma$ process on the threshold s_0 and Borel parameter M^2 .

-
- [1] H. Y. Gao, *Int. J. Mod. Phys. E* **12**, 1 (2003), [Erratum: *Int.J.Mod.Phys.E* 12, 567 (2003)], [arXiv:nucl-ex/0301002](#) .
- [2] S. Pacetti, R. Baldini Ferroli, and E. Tomasi Gustafsson, *Phys. Rept.* **550-551**, 1 (2015).
- [3] K. G. Wilson, *Phys. Rev. D* **10**, 2445 (1974).
- [4] M. Luscher, S. Sint, R. Sommer, P. Weisz, and U. Wolff, *Nucl. Phys. B* **491**, 323 (1997), [arXiv:hep-lat/9609035](#) .
- [5] G. S. Bali, *Phys. Rept.* **343**, 1 (2001), [arXiv:hep-ph/0001312](#) .
- [6] S. Navas *et al.* (Particle Data Group), *Phys. Rev. D* **110**, 030001 (2024).
- [7] A. E. Asratian *et al.*, *Phys. Lett. B* **257**, 525 (1991).
- [8] S. Abachi *et al.*, *Phys. Lett. B* **212**, 533 (1988).

- [9] J. Gronberg et al. (CLEO), *Phys. Rev. Lett.* **75**, 3232 (1995), [arXiv:hep-ex/9508001](#) .
- [10] H. Albrecht et al. (ARGUS), *Z. Phys. C* **66**, 63 (1995).
- [11] M. Ablikim et al. (BESIII), *Phys. Rev. D* **91**, 031101 (2015), [arXiv:1412.4566 \[hep-ex\]](#) .
- [12] M. Ablikim et al. (BESIII), *Phys. Rev. D* **107**, 032011 (2023), [arXiv:2212.13361 \[hep-ex\]](#) .
- [13] C. Edwards et al., *Phys. Rev. Lett.* **48**, 70 (1982).
- [14] S. K. Choi et al. (Belle), *Phys. Rev. Lett.* **89**, 102001 (2002), [Erratum: *Phys.Rev.Lett.* 89, 129901 (2002)], [arXiv:hep-ex/0206002](#) .
- [15] M. Ablikim et al. (BESIII), *Phys. Rev. D* **109**, 032004 (2024), [arXiv:2309.14689 \[hep-ex\]](#) .
- [16] S. Godfrey and N. Isgur, *Phys. Rev. D* **32**, 189 (1985).
- [17] T. Barnes, S. Godfrey, and E. S. Swanson, *Phys. Rev. D* **72**, 054026 (2005), [arXiv:hep-ph/0505002](#) .
- [18] S. Godfrey and K. Moats, *Phys. Rev. D* **93**, 034035 (2016), [arXiv:1510.08305 \[hep-ph\]](#) .
- [19] J. L. Goity and W. Roberts, *Phys. Rev. D* **64**, 094007 (2001), [arXiv:hep-ph/0012314](#) .
- [20] T. Peng and B. Q. Ma, *Eur. Phys. J. A* **48**, 66 (2012), [arXiv:1204.0863 \[hep-ph\]](#) .
- [21] H. M. Choi and C. R. Ji, *Phys. Rev. D* **59**, 074015 (1999), [arXiv:hep-ph/9711450](#) .
- [22] G. Li and Q. Zhao, *Phys. Lett. B* **670**, 55 (2008), [arXiv:0709.4639 \[hep-ph\]](#) .
- [23] G. Li and Q. Zhao, *Phys. Rev. D* **84**, 074005 (2011), [arXiv:1107.2037 \[hep-ph\]](#) .
- [24] T. M. Aliev, E. Iltan, and N. K. Pak, *Phys. Lett. B* **334**, 169 (1994).
- [25] H. G. Dosch and S. Narison, *Phys. Lett. B* **368**, 163 (1996), [arXiv:hep-ph/9510212](#) .
- [26] S. L. Zhu, W. Y. P. Hwang, and Z. S. Yang, *Mod. Phys. Lett. A* **12**, 3027 (1997), [arXiv:hep-ph/9610412](#) .
- [27] J. Lu, G. L. Yu, Z. G. Wang, and B. Wu, *Phys. Lett. B* **852**, 138624 (2024), [arXiv:2401.00669 \[hep-ph\]](#) .
- [28] J. J. Dudek, R. Edwards, and C. E. Thomas, *Phys. Rev. D* **79**, 094504 (2009), [arXiv:0902.2241 \[hep-ph\]](#) .
- [29] B. Owen, W. Kamleh, D. Leinweber, B. Menadue, and S. Mahbub, *Phys. Rev. D* **91**, 074503 (2015), [arXiv:1501.02561 \[hep-lat\]](#) .
- [30] Y. Meng, J. L. Dang, C. Liu, Z. Liu, T. Shen, H. Yan, and K. L. Zhang, *Phys. Rev. D* **109**, 074511 (2024), [arXiv:2401.13475 \[hep-lat\]](#) .
- [31] B. Colquhoun, L. J. Cooper, C. T. H. Davies, and G. P. Lepage (Particle Data Group, HPQCD, (HPQCD Collaboration)‡), *Phys. Rev. D* **108**, 014513 (2023), [arXiv:2305.06231 \[hep-lat\]](#) .
- [32] C. Alexandrou, L. Leskovec, S. Meinel, J. Negele, S. Paul, M. Petschlies, A. Pochinsky, G. Rendon, and S. Syritsyn, *Phys. Rev. D* **98**, 074502 (2018), [Erratum: *Phys.Rev.D* 105, 019902 (2022)], [arXiv:1807.08357 \[hep-lat\]](#) .
- [33] F. X. Lee, S. Moerschbacher, and W. Wilcox, *Phys. Rev. D* **78**, 094502 (2008), [arXiv:0807.4150 \[hep-lat\]](#) .
- [34] D. Becirevic and B. Haas, *Eur. Phys. J. C* **71**, 1734 (2011), [arXiv:0903.2407 \[hep-lat\]](#) .
- [35] S. P. Guo, Y. J. Sun, W. Hong, Q. Huang, and G. H. Zhao, *Nucl. Phys. B* **955**, 115053 (2020), [arXiv:1912.00836 \[hep-ph\]](#) .
- [36] B. Pullin and R. Zwicky, *JHEP* **09**, 023 (2021), [arXiv:2106.13617 \[hep-ph\]](#) .
- [37] T. M. Aliev, A. Ozpineci, and M. Savci, *Phys. Lett. B* **678**, 470 (2009), [arXiv:0902.4627 \[hep-ph\]](#) .
- [38] T. M. Aliev, S. Bilmis, and M. Savci, *Phys. Rev. D* **101**, 054009 (2020), [arXiv:1912.05988 \[hep-ph\]](#) .
- [39] M. Anselmino, M. Genovese, and E. Predazzi, *Phys. Rev. D* **44**, 1597 (1991).

- [40] K. T. Chao, Y. F. Gu, and S. F. Tuan, *Commun. Theor. Phys.* **25**, 471 (1996).
- [41] H. Wang and C. Z. Yuan, *Chin. Phys. C* **46**, 071001 (2022), [arXiv:2112.08584 \[hep-ph\]](#) .
- [42] M. A. Shifman, A. I. Vainshtein, and V. I. Zakharov, *Nucl. Phys. B* **147**, 385 (1979).
- [43] V. M. Braun and I. E. Filyanov, *Z. Phys. C* **44**, 157 (1989).
- [44] A. Cerqueira Jr, B. O. Rodrigues, M. E. Bracco, and C. M. Zanetti, *Braz. J. Phys.* **52**, 12 (2022), [arXiv:2112.03146 \[hep-ph\]](#) .
- [45] Z. X. Zhao, X. Y. Sun, F. W. Zhang, Y. P. Xing, and Y. T. Yang, *Phys. Rev. D* **108**, 116008 (2023), [arXiv:2103.09436 \[hep-ph\]](#) .
- [46] Y. Q. Peng and M. Z. Yang, *Mod. Phys. Lett. A* **35**, 2050187 (2020), [arXiv:1909.03370 \[hep-ph\]](#) .
- [47] K. Azizi, M. Bayar, A. Ozpineci, and Y. Sarac, *Phys. Rev. D* **82**, 076004 (2010), [arXiv:1008.0202 \[hep-ph\]](#) .
- [48] W. Lucha, D. Melikhov, and S. Simula, *Phys. Lett. B* **765**, 365 (2017), [arXiv:1609.05050 \[hep-ph\]](#) .
- [49] Z. G. Wang, *Eur. Phys. J. C* **75**, 427 (2015), [arXiv:1506.01993 \[hep-ph\]](#) .
- [50] B. D. Wan and Y. R. Wang, *Eur. Phys. J. A* **60**, 179 (2024).
- [51] S. S. Agaev, K. Azizi, and H. Sundu, *Phys. Lett. B* **858**, 139042 (2024), [arXiv:2407.14961 \[hep-ph\]](#) .
- [52] Z. G. Wang, *Nucl. Phys. B* **1007**, 116661 (2024), [arXiv:2407.08759 \[hep-ph\]](#) .
- [53] U. Özdem, *J. Phys. G* **46**, 035003 (2019), [arXiv:1804.10921 \[hep-ph\]](#) .
- [54] U. Özdem, *Eur. Phys. J. A* **58**, 46 (2022).
- [55] J. J. Dudek, R. G. Edwards, and D. G. Richards, *Phys. Rev. D* **73**, 074507 (2006), [arXiv:hep-ph/0601137](#) .
- [56] Y. J. Sun, X. G. Wu, F. Zuo, and T. Huang, *Eur. Phys. J. C* **67**, 117 (2010), [arXiv:0911.0963 \[hep-ph\]](#) .
- [57] G. P. Lepage and S. J. Brodsky, *Phys. Rev. D* **22**, 2157 (1980).
- [58] A. Khodjamirian, R. Ruckl, S. Weinzierl, C. W. Winhart, and O. I. Yakovlev, *Phys. Rev. D* **62**, 114002 (2000), [arXiv:hep-ph/0001297](#) .
- [59] W. Y. Wang, Y. L. Wu, and M. Zhong, *Phys. Rev. D* **67**, 014024 (2003), [arXiv:hep-ph/0205157](#) .
- [60] A. Khodjamirian, T. Mannel, and M. Melcher, *Phys. Rev. D* **70**, 094002 (2004), [arXiv:hep-ph/0407226](#) .
- [61] H. M. Choi and C. R. Ji, *Phys. Rev. D* **75**, 034019 (2007), [arXiv:hep-ph/0701177](#) .
- [62] P. Ball, V. M. Braun, and A. Lenz, *JHEP* **05**, 004 (2006), [arXiv:hep-ph/0603063](#) .
- [63] G. S. Bali, V. M. Braun, S. Bürger, M. Göckeler, M. Gruber, F. Hutzler, P. Korcyl, A. Schäfer, A. Sternbeck, and P. Wein (RQCD), *JHEP* **08**, 065 (2019), [Addendum: *JHEP* 11, 037 (2020)], [arXiv:1903.08038 \[hep-lat\]](#) .
- [64] H. M. Choi and C. R. Ji, *Phys. Rev. D* **75**, 034019 (2007), [arXiv:hep-ph/0701177](#) .
- [65] S. B. Wu, H. J. Tian, Y. L. Yang, W. Cheng, H. B. Fu, and T. Zhong, *Eur. Phys. J. C* **85**, 552 (2025), [arXiv:2501.02694 \[hep-ph\]](#) .
- [66] F. E. Serna, R. C. da Silveira, J. J. Cobos Martinez, B. El Bennich, and E. Rojas, *Eur. Phys. J. C* **80**, 955 (2020), [arXiv:2008.09619 \[hep-ph\]](#) .
- [67] T. Huang and F. Zuo, *Eur. Phys. J. C* **51**, 833 (2007), [arXiv:hep-ph/0702147](#) .
- [68] T. Huang, B. Q. Ma, and Q. X. Shen, *Phys. Rev. D* **49**, 1490 (1994), [arXiv:hep-ph/9402285](#) .
- [69] F. G. Cao and T. Huang, *Phys. Rev. D* **59**, 093004 (1999), [arXiv:hep-ph/9711284](#) .
- [70] T. Huang and X. G. Wu, *Phys. Rev. D* **70**, 093013 (2004), [arXiv:hep-ph/0408252](#) .

- [71] T. Huang and X. G. Wu, *Int. J. Mod. Phys. A* **22**, 3065 (2007), [arXiv:hep-ph/0606135](#) .
- [72] A. E. Bondar and V. L. Chernyak, *Phys. Lett. B* **612**, 215 (2005), [arXiv:hep-ph/0412335](#) .
- [73] H. M. Choi, *Phys. Rev. D* **75**, 073016 (2007), [arXiv:hep-ph/0701263](#) .
- [74] A. J. Arifi, H. M. Choi, C. R. Ji, and Y. Oh, *Phys. Rev. D* **106**, 014009 (2022), [arXiv:2205.04075 \[hep-ph\]](#) .
- [75] S. Aoki *et al.*, *Eur. Phys. J. C* **77**, 112 (2017), [arXiv:1607.00299 \[hep-lat\]](#) .
- [76] D. Ebert, R. N. Faustov, and V. O. Galkin, *Phys. Lett. B* **537**, 241 (2002), [arXiv:hep-ph/0204089](#) .
- [77] M. Priyadarsini, P. C. Dash, S. Kar, S. P. Patra, and N. Barik, *Phys. Rev. D* **94**, 113011 (2016).
- [78] T. M. Aliev, D. A. Demir, E. Iltan, and N. K. Pak, *Phys. Rev. D* **54**, 857 (1996), [arXiv:hep-ph/9511362](#) .
- [79] P. Colangelo, F. De Fazio, and G. Nardulli, *Phys. Lett. B* **316**, 555 (1993), [arXiv:hep-ph/9307330](#) .
- [80] B. Mohan, C. M. A., and R. Dhir, (2025), [arXiv:2506.10560 \[hep-ph\]](#) .
- [81] R. Bonnaz, B. Silvestre Brac, and C. Gignoux, *Eur. Phys. J. A* **13**, 363 (2002), [arXiv:hep-ph/0101112](#) .
- [82] J. L. Li and D. Y. Chen, *Chin. Phys. C* **46**, 073106 (2022), [arXiv:2212.11861 \[hep-ph\]](#) .
- [83] K. K. Zhang, W. X. Zhang, and D. Jia, *Phys. Rev. D* **112**, 054008 (2025), [arXiv:2503.14987 \[hep-ph\]](#) .
- [84] W. N. Liu, W. X. Zhang, and F. Q. Dou, *Phys. Rev. D* **111**, 114031 (2025), [arXiv:2501.12727 \[hep-ph\]](#) .
- [85] Y. L. Zhang, S. Cheng, J. Hua, and Z. J. Xiao, *Phys. Rev. D* **92**, 094031 (2015), [arXiv:1510.05108 \[hep-ph\]](#) .